International Journal of Computational Intelligence Systems and Applications. Volume 9, Issue 1, (2022) 25-36
http://www.cayley-nielson.com/ijcisa/

Image De-noising on Strip Steel Surface Defect Using WCROMP Algorithm

Dongyan Cui
School of Artificial Intelligence, North China University of Science and Technology, Tangshan, Hebei, China
E-mail: *cdy_xxz@163.com*

Abstract

De-noising for the strip steel surface defect image is conductive to the accurate detection of the strip steel surface defects. In order to filter the Gaussian noise and salt and pepper noise of strip steel surface defect images, an improved Regularized Orthogonal Matching Pursuit algorithm(ROMP) was applied to defect image de-noising in this paper. First, the Weighted Correlation ROMP(WCROMP) algorithm was described. Then, three typical surface defects (scratch, scar, surface upwarping) images were selected as the experimental samples. Last, detailed experimental tests were carried out to the strip steel surface defect image de-noising. Through comparison and analysis of the test results, the Peak Signal to Noise Ratio(PSNR) value of the proposed algorithm is higher compared with other traditional de-noising algorithm, and the running time of the proposed algorithm is only 24.1% of that of traditional Orthogonal Matching Pursuit (OMP) algorithms. Therefore, it has better de-noising effect and can meet the requirements of real-time image processing.

Keywords: compressive sensing; strip surface defects; image de-noising; Weighted Correlation Regularized Orthogonal Matching Pursuit

1. Introduction

Image noise reduction is a classical problem in image processing which has over 50 years of research history [1-2], and still is a hot topic. The strip steel surface defect images in the process of collection, acquisition and transmission will be polluted to some extent by visible or invisible noise, also due to the unstable light, camera vibration and other factors etc. Therefore, it is necessary to carry out the noise processing of the collected images.

A large number of studies have been carried out on the surface defect image de-noising at home. In 2008, Liu Weiwei, Yun Hui Yan et al of Northeastern University put forward an image de-noising method based on local similarity analysis and neighborhood noise evaluation. The experimental results show that the de-noising effect of the novel filter is better than that of other classical filter [3]; In 2009, Weiwei Liu, Yun Hui Yan et al also put forward a wavelet-based image filtering method by virtue of anisotropic diffusion, which can effectively filter off the unnecessary texture background and preserve the valuable information in details [4]; In 2010, Bo Tang et al studied the rules of strip steel surface defects image de-noising based on wavelet threshold. Experimental results show that the wavelet threshold de-noising method can improve the image signal-to-noise ratio and improve the image quality [5]; In 2010, Yunhui Yan of Northeastern University proposed the impulse noise filtering method based on threshold theory. The de-noising effect is better than that of the traditional filtering method [6]; In 2012, Hao Xu of Wuhan University of Science and

Technology proposed the method of surface defect of strip steel based on mathematical morphology, which could detect small defect edge under strong noise and own strong noise immunity [7].

From the above, the existing strip steel surface defect image de-noising methods mainly focused on the traditional filtering method, which can be divided into two categories: One is the spatial domain processing, which mainly uses a variety of smooth templates and images for convolution processing, so as to achieve the purpose of noise reduction or elimination; The other is the transform domain processing, first of all, the image is transformed, and then with the appropriate frequency band pass filter for filtering processing, and finally to get the image through the inverse transform. In the existing theory, the original signal is mostly projected to a certain transformation space, and the sparsity of the coefficient in the projection domain is as a fundamental basis. While the existence of noise affected the sparsity of signals in the transform space. So the optimization method is used to restore the signal, if only a single sparse constraint principle is used, it is difficult to accurately reconstruct the original signal. In this case, compressive sensing theory still may take other effective method of reconstructing. Numerous studies show that the reconstruction algorithm based on compression perception theory is applied in signal de-noising can achieve good effect [8-10]. Donoho [11-12], Candes [13-17], Tao [16-17] and Romberg [15-17] and other scientists initially put forward the concept of compressed sensing from sparse signal decomposition and approximation theory in 2004, followed by a large number of relevant theoretical research. During this period, Candes proved that the original signal can be accurately reconstructed from partial Fourier transform coefficients in 2006, which laid a solid theoretical foundation for the compression perception theory. They formally announced the theory on the basis of relevant research in 2006. D. L. Donoho proposed the compressive sensing de-noising method for the noise suppression based on the basis pursuit (BP) algorithm. When the sparsity of the signal is known, least absolute shrinkage and selection operator(LASSO) is proposed to restore and de-noise the signal effectively [11]. M.A.T. Figueiredo proposed the gradient projection for sparse reconstruction(GPSR)algorithm based on the L1 norm. The method does not need to consider the noise distribution and the sparsity of the original signal, not only more universal than the previous method, and obtain the good effect of de-noising [18].

The compressed perception theory is introduced into the strip steel surface defect image preprocessing, which is rarely mentioned in the literature at home and abroad. Therefore, In this paper, the Weighted Correlation ROMP algorithm was applied to the strip steel surface defect image de-noising, which has better de-noising effect and shorter running time compared with traditional median filtering, wavelet threshold method and traditional compressed sensing algorithm.

2. Description of weighted correlation ROMP algorithm

Needell et al proposed the regularized orthogonal matching pursuit algorithm (ROMP) based on the orthogonal matching pursuit (OMP) [19-21]. All matrices satisfied the restricted isometry condition and all sparse signals can be reconstructed.

The algorithm was improved based on ROMP algorithm. The selection of atomic index set for the first time was using weighted correlation coefficient, not only considering the correlation coefficient of the current iteration, also considering the correlation coefficient of the last iteration, and expanding the selection scope of index value. Weighted formula is as follows.

$$g^t = \alpha g + \beta g^{t-1}$$

$$\text{s.t. } g = A^T r^{t-1}, 0 < \alpha < 1, 0 < \beta < 1, \alpha + \beta = 1 \quad (1)$$

The pseudo code of algorithm is as follows.

Input:(1)measurement matrix y , $y \in R^N$;(2)$M \times N$ dimensional sensing matrix $A = \phi\psi$ $A = \phi\psi$;(3) sparsity level K of the signal(the number of nonzero elements in x).

Output： N dimensional reconstructed signal(sparse approximation signal) $\hat{x} \in R^N$ $\hat{x} \in R^N$。

Initialize： $r_0 = y, \Lambda_0 = \phi, A_0 = \phi$ $r_0 = y, \Lambda_0 = \emptyset, A_0 = \emptyset$

Iteration：

step(1): Calculate: $g = abs[A^T r_{t-1}]$ $g = abs[A^T r_{t-1}]$(which is: $\langle r_{t-1}, \alpha_j \rangle, 1 \le j \le N$);

step(2): Obtain $u = |g^t|$ $u = |g^t|$according to formula (1),choose a set J of the K biggest or nonzero values, which corresponds to the column number of A and construct a set J ;

step(3): Regularize: $|u_i| \le 2|u_j|$ $|u(i)| \le 2|u(j)|$, for all $i, j \in J_0$ $i, j \in J_0$,Among all subset J_0 J_0,choose J_0 J_0 with the maximal energy $\sum_j |u(j)|^2, j \in J_0$ $\sum_j |u(j)|^2, j \in J_0$;

step(4): $\Lambda_t = \Lambda_{t-1} \bigcup J_0$ $\Lambda_t = \Lambda_{t-1} \cup J_0$, $A_t = A_{t-1} \bigcup \alpha_j$ $A_t = A_{t-1} \cup \alpha_j$(,for all $j \in J_0$ $j \in J_0$);

step(5): Calculate the least squares solution of $y = A_t \theta_t$ $y = A_t \theta_t$: $\hat{\theta}_t = \arg\min_{\theta_t} \|y - A_t \theta_t\| = (A_t^T A_t)^{-1} A_t^T y$ $\hat{\theta}_t = \arg\min_{\theta_t} \|y - A_t \theta_t\| = (A_t^T A_t)^{-1} A_t^T y$;

step(6): Update residual: $r_t = y - A_t \hat{\theta}_t = y - A_t (A_t^T A)^{-1} A_t^T y$ $r_t = y - A_t \hat{\theta}_t = y - A_t (A_t^T A)^{-1} A_t^T y$

step(7): $t = t + 1$, if $t \le K$ $t \le K$, then return step (1), if $t > K$ $t > K$ or $\|\Lambda_t\|_0 \ge 2K$ $\|\Lambda_t\|_0 \ge 2K$($\|\Lambda_t\|_0$ represents the number of elements in the set or residua $r_t = 0$ $r_t = 0$,then the iteration stop, and enter step (7);

step(8): $\hat{\theta}_t$ $\hat{\theta}_t$ has nonzero entries at Λ_t Λ_t , the value is respectively $\hat{\theta}_t$ $\hat{\theta}_t$ obtained from reconstruction；

step(9): reconstructed the signal ： $\hat{x} = \psi \hat{\theta}$ $\hat{x} = \Psi\hat{\theta}$.

3. De-noising model based on the weighted correlation ROMP algorithm

Assuming that the received image signal is $g(x, y)$ $g(x, y)$, which is contaminated by noise. The clean image is $f(x, y)$. The additive noise is $n(x, y)$ $n(x, y)$ .Then the additive noise model is

$g(x,y)=f(x,y)+n(x,y)$ g(x, y) = f(x, y) + n(x, y). When the signal is disturbed by multiplicative noise, the model is expressed as:

$$g(x,y)=f(x,y)\left(1+n(x,y)\right)=f(x,y)+f(x,y)n(x,y) \tag{2}$$

Where, the output signal of the second term is the result of multiplying the noise, which is affected by f(x, y). The bigger f(x, y), the bigger the noise. According to the theory of compressive sensing, the following results can be obtained.

$$g(x,y)=f(x,y)+n(x,y)=\phi\alpha \tag{3}$$

Where, α α is a sparse representation of the transformed image. In this way, we can recover the original image by estimating the sparse representation of the clean image so as to achieve the purpose of removing the noise.

The de-noising model based on the compressive sensing model is as follows.

$$\alpha=\arg\min\|\alpha\|_0$$

$$\text{s.t. } \|\Phi\alpha-g\|_2^2\le T \tag{4}$$

Specific algorithm is described as:

(1) Add noise to the clean image.

(2) Obtain the sparse representation of noisy image.

(3) Calculate the optimal solution of $\alpha=\arg\min\|\alpha\|_0$ α = arg min‖α‖0 using weighted correlation ROMP algorithm and remove noise.

(4) Reconstruct the image.

4. Experimental results and discussion

The quality of the strip steel surface image is affected by the illumination conditions, the steel quality and the interference of the environment. De-noising is an important step in surface defect detection technology. The noise mainly comes from image acquisition and image transmission process, mainly as the Gaussian noise, salt and pepper noise and impulse noise. Three kinds of strip steel defect images (scratch, scar, surface upwarping) are selected in this paper, and the noise type is Gaussian noise and salt and pepper noise

The hardware requirement of the experiment is as follows: CPU is Intel Core i5 760 2.8 GHz, 2 GB memory, and the software platform is the Windows7 operating system, and the simulation software is Matlab2016a.

4.1. Simulation experiment 1: Strip steel defect image de-noising polluted by Gaussian noise

Firstly, Table1 shows the de-noising results of three types of defects (scratch, scar, facial warping) under Gaussian noise using Median filter, Mean filter, Wiener filter, Wavelet, OMP, StOMP Cosamp, and the

proposed algorithm(WCROMP). The sampling rate is 0.5, The transformation matrix is the DWT matrix. The Gaussian noise mean is 0 and variance is 0.1, 0.01, 0.005 respectively, as shown in Table 1 below. Type of experiment defects respectively are scratch, scar and surface upwarping. 3 * 3 templates are selected in mean filter and median filter for processing. Wiener filtering using two-dimensional adaptive filtering, the filter window size is 3] [3, wavelet denoising coif2 wavelet function to select the image of the 2-layer decomposition. The experimental results are shown in Tab. 1.

Tab. 1. the de-noising effect comparison of various algorithms with different intensity Gaussian noise

Noise	Algorithm	scratch		Scar		Surface upwarping	
		PSNR	*Time*	*PSNR*	*Time*	*PSNR*	*Time*
0.1	Median	17.4003	0.3590	17.4078	0.3590	17.1443	0.3590
	Mean	19.3258	0.3580	18.6787	0.3460	18.9338	0.3430
	Wiener	24.0654	0.3430	24.0659	0.3810	24.0656	0.3750
	Wavelet	26.7816	0.4380	26.6659	0.4300	26.5330	0.4050
	OMP	15.0354	13.1650	15.2636	12.4310	15.1019	12.5560
	StOMP	9.2337	3.8170	9.6184	4.2600	9.5914	0.8733
	CoSaMP	7.9872	7.5220	8.0573	7.5410	7.9607	7.8940
	ROMP	14.9193	3.0880	15.0791	3.0810	14.9364	3.1040
	WCROMP	26.8728	2.9952	26.7509	2.9952	26.5816	3.1512
0.01	Median	26.7837	0.6870	26.4997	0.3900	25.3972	0.3900
	Mean	24.6074	0.3520	24.5073	0.3700	23.311	0.3700
	Wiener	24.0654	0.3800	24.0655	0.3600	24.0657	0.3430
	Wavelet	26.7988	0.4200	26.6642	0.3740	26.5000	0.3800
	OMP	24.1334	12.9040	24.1121	12.4770	23.8210	12.8820
	StOMP	18.2092	0.3495	18.2085	4.4010	17.8416	3.9710
	CoSaMP	15.3426	7.6610	14.9957	7.7920	14.7124	7.6910
	ROMP	22.2239	3.2720	21.6963	3.1500	21.3672	3.0890
	WCROMP	29.9563	3.0888	29.2152	3.0420	29.3068	2.9952
0.005	Median	29.2534	0.3700	28.8605	0.3750	26.9201	0.4000
	Mean	25.3331	0.3430	24.8847	0.3400	24.1503	0.3600
	Wiener	24.0654	0.3680	24.0654	0.3700	24.0661	0.3750
	Wavelet	26.8362	0.4380	26.6714	0.3730	26.4840	0.3900
	OMP	27.0289	12.3110	26.8914	12.8130	26.4759	12.6230
	StOMP	21.3373	4.1630	21.4450	4.2220	20.3319	4.1460
	CoSaMP	17.3229	7.8340	17.0306	7.6520	15.9426	7.5720
	ROMP	26.5296	3.1400	24.7132	3.1760	22.3631	3.1270
	WCROMP	33.6600	3.0576	32.3062	3.1356	32.5256	3.0108

From the experimental data and experimental results in Tab. 1, the PSNR value and the running time is higher than the OMP algorithm, CoSaMP algorithm StOMP algorithm and ROMP algorithm using the proposed method to de-noise the strip steel surface defect image. Although the running time is slightly higher than that of the traditional algorithms, such as Median filter, Mean filter, Winer filter, Wavelet. But compared with the OMP algorithm and the CoSaMP algorithm, the running time is greatly reduced, about

24.1% of the OMP algorithm. In terms of training time, although the WCROMP algorithm takes a little longer than the traditional filter algorithms, there is no impact on the real-time performance of the defect detection classification because the training modeling is an off-line processing. Experiments show that, considering the de-noising effect and the running time, the performance of this WCROMP algorithm to handle strip surface defect image Gaussian noise pollution is optimal. Therefore, this algorithm is selected in this paper, and the effect of image de-noising is compared with other traditional de-noising methods.

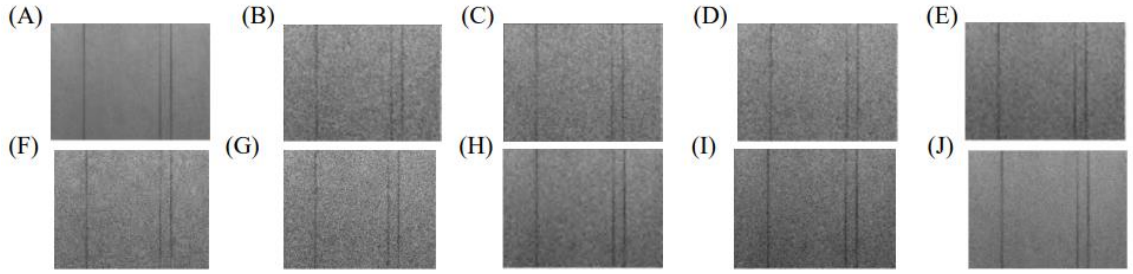

Fig. 1. Scratch(Gaussian noise with mean 0 and variance 0.01)(A)The original image of scratch (B) Median filtering image (C) Mean filtering image(D)Wiener filtering image (E) Wavelet de-noising image (F)OMP de-noising image(G) StOMP De-noising image (H) CoSaMP De-noising image (I) ROMP De-noising image(J) WCROMP De-noising image

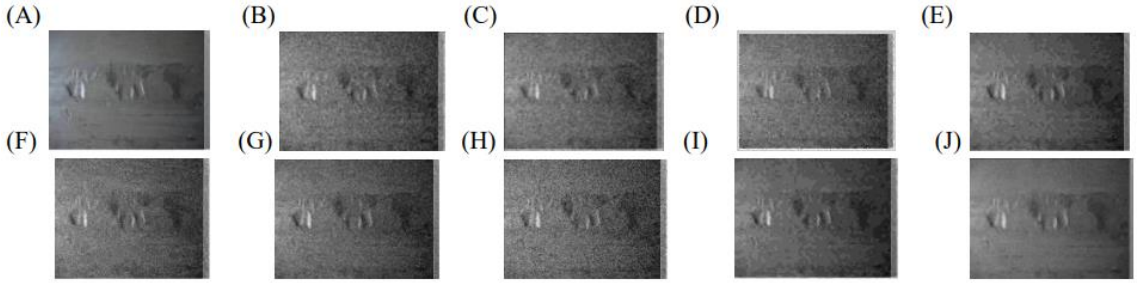

Fig. 2. Scar(Gaussian noise with mean 0 and variance 0.01)(A)The original image of scratch (B) Median filtering image (C) Mean filtering image(D)Wiener filtering image (E) Wavelet de-noising image (F)OMP de-noising image(G) StOMP De-noising image (H) CoSaMP De-noising image (I) ROMP De-noising image(J) WCROMP De-noising image

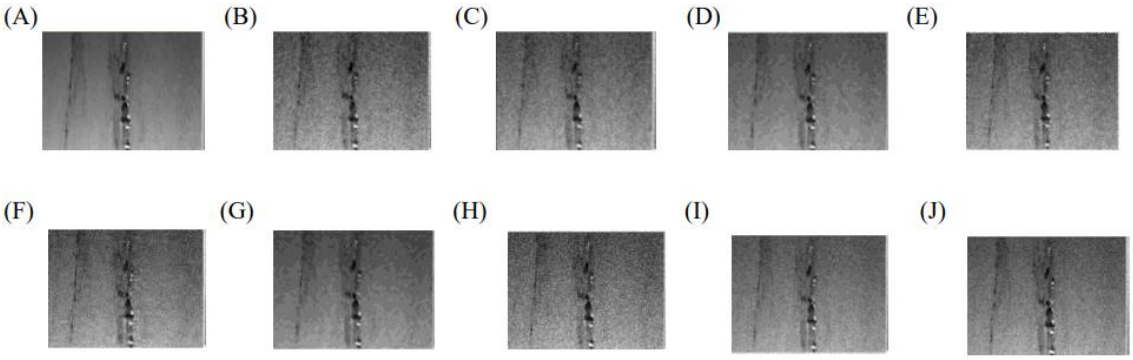

Fig. 3. Surface upwarping(Gaussian noise with mean 0 and variance 0.01)(A)The original image of scratch (B) Median filtering image (C) Mean filtering image(D)Wiener filtering image (E) Wavelet de-noising image

(F)OMP de-noising image(G) StOMP De-noising image (H) CoSaMP De-noising image (I) ROMP De-noising image(J) WCROMP De-noising image

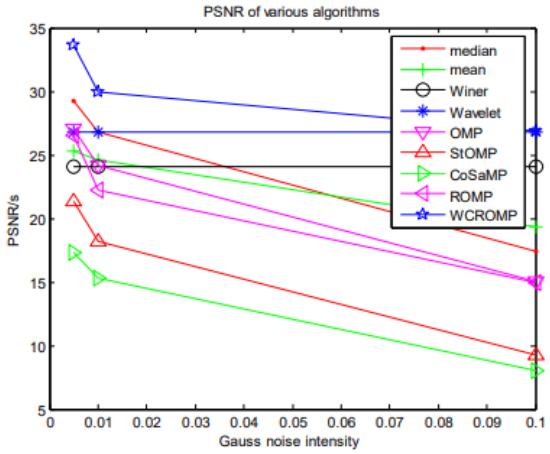

(A)

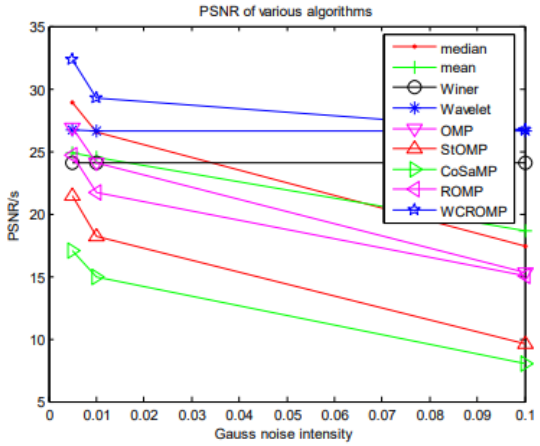

(B)

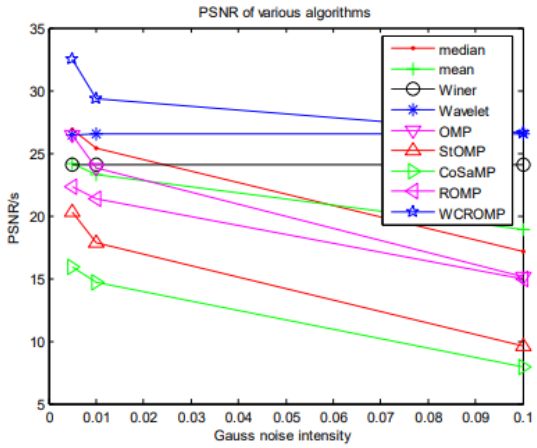

(C)

Fig. 4. The PSNR comparison curve obtained by using various de-noising algorithms(A)The PSNR curve of scratch image (B) The PSNR curve of scar image (C) The PSNR curve of surface upwarping image

Considering the length of this paper, we only show part of the processing images. Fig. 1(A)-(J) to Fig. 3(A)-(J) are respectively the results of three kinds of defects when the Gaussian noise mean is 0 and the variance is 0.01.

Fig. 4 (A)-(C) are respectively the PSNR comparison curve of three kinds of defects noisy images obtained by using various de-noising algorithms.

As shown in Fig. 4, the PSNR values of the various algorithms are all decreased with the increasing of the noise intensity. Compared with other traditional de-noising methods, the proposed method in this paper has higher PSNR value, that is, the effect is better.

4.2. Simulation experiment 2: Strip steel defect image de-noising polluted by salt and pepper noise

Type of defects are respectively scratch, scar and surface upwarping in the experiment. Salt and pepper noise intensity are 0.1, 0.01,0.005. 3*3 templates is selected in mean filter and median filter for processing. Fig. 5(A)-(J) to Fig. 7(A)-(J) are respectively the results of three kinds of defects de-noising images.

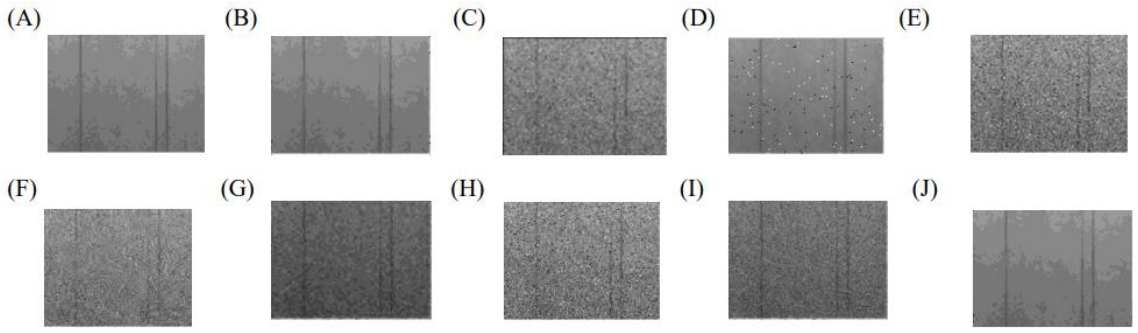

Fig. 5. Scratch(Salt and pepper noise intensity is 0.1) (A)The original image of scratch (B) Median filtering image (C) Mean filtering image(D)Wiener filtering image (E) Wavelet de-noising image (F)OMP de-noising image(G) StOMP De-noising image (H) CoSaMP De-noising image (I) ROMP De-noising image(J) WCROMP De-noising image

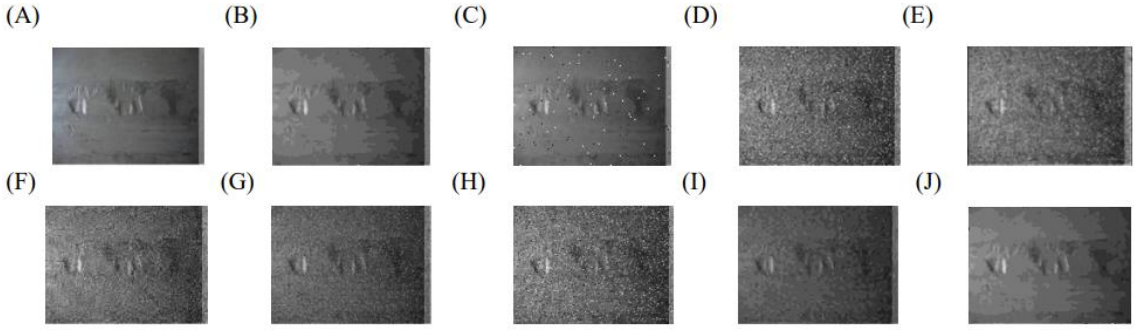

Fig. 6. Scar(Salt and pepper noise intensity is 0.1) (A)The original image of scratch (B) Median filtering image (C) Mean filtering image(D)Wiener filtering image (E) Wavelet de-noising image (F)OMP de-noising image(G) StOMP De-noising image (H) CoSaMP De-noising image (I) ROMP De-noising image(J) WCROMP De-noising image

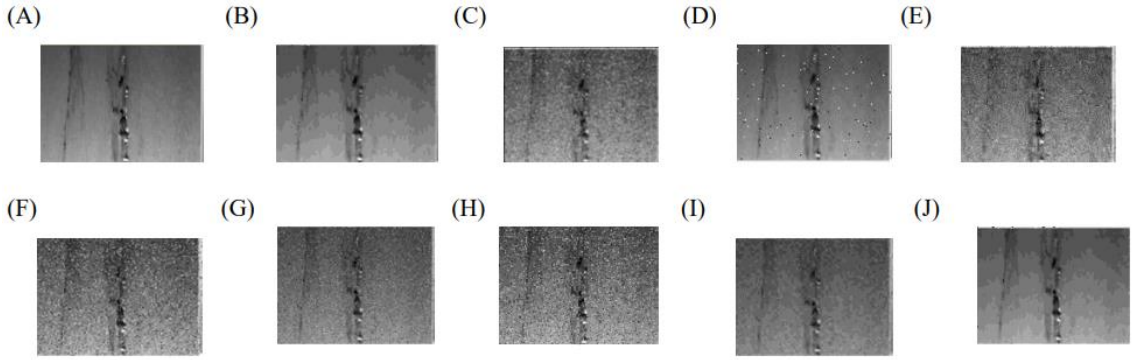

Fig. 7. Surface upwarping(Salt and pepper noise intensity is 0.1) (A)The original image of scratch (B) Median filtering image (C) Mean filtering image(D)Wiener filtering image (E) Wavelet de-noising image (F)OMP de-noising image(G) StOMP De-noising image (H) CoSaMP De-noising image (I) ROMP De-noising image(J) WCROMP De-noising image

Tab. 2 shows the PSNR values of three kinds of defects using various de-noising algorithms (Salt and pepper noise intensity is 0.1).

Tab. 2. The de-noising effect comparison of various algorithms with different intensity Salt and Pepper noise

Noise	Algorithm	scratch		Scar		Surface upwarping	
		PSNR	*Time*	*PSNR*	*Time*	*PSNR*	*Time*
0.1	Median	32.4615	0.3870	30.7089	0.3950	27.2937	0.3870
	Mean	22.7412	0.4350	22.0239	0.4150	21.8199	0.4500
	Wiener	24.0659	0.4170	24.0657	0.3830	24.0664	0.3820
	Wavelet	23.4522	0.7920	23.2282	0.4080	22.9576	0.4000
	OMP	22.1598	12.6910	23.2882	12.3680	22.1627	13.3040
	StOMP	14.2820	4.4550	13.8143	4.0180	14.0231	3.8950
	CoSaMP	12.3928	7.3180	11.8036	7.2760	11.7297	7.2200
	ROMP	18.6954	3.2630	15.0287	2.8160	18.7413	2.8070
	WCROMP	33.5687	3.0714	31.1205	2.7089	29.2302	2.7780
0.01	Median	36.3120	0.4950	34.7921	0.3820	29.7290	0.4050
	Mean	26.3138	0.3900	25.4130	0.4070	24.4165	0.4150
	Wiener	24.0662	0.4120	24.0661	0.3800	24.0670	0.3820
	Wavelet	26.6945	0.3770	26.6336	0.3830	26.5667	0.4120
	OMP	32.4924	12.0001	30.9695	11.9400	30.6486	12.3880
	StOMP	24.0350	3.8520	23.7123	3.8000	22.3026	3.880
	CoSaMP	18.9369	7.3580	17.8524	7.1750	18.0432	7.1250
	ROMP	27.3696	2.9760	23.0203	3.0120	26.4229	3.0050
	WCROMP	37.3122	3.0800	36.5890	2.9080	34.7397	2.9860
0.005	Median	36.4572	0.4080	34.8081	0.3820	29.7310	0.4000
	Mean	26.6779	0.3780	25.6082	0.3980	24.8591	0.3750
	Wiener	24.0656	0.3750	24.0655	0.3930	24.0669	0.3950
	Wavelet	40.9801	0.4070	40.0989	0.3880	38.0236	0.3850

OMP	35.9337	12.2280	34.4295	12.0820	32.7035	14.5890
StOMP	26.3848	3.8050	25.7025	3.8030	23.7764	4.5300
CoSaMP	20.4533	7.9060	18.7628	7.1640	18.3959	7.3380
ROMP	33.2296	2.9150	25.3678	3.1790	29.8547	2.9580
WCROMP	42.4640	3.0802	40.7194	3.0880	38.1562	2.9010

Figure 8 (a)-(c) are respectively the PSNR comparison curve of three kinds of defects noisy images obtained by using various de-noising algorithms.

As shown in Tab. 2 and Fig. 8, the PSNR values of the various algorithms are all decreased with the increasing of the noise intensity. The median filtering method is very effective for the de-noising of salt and pepper noise. Compared with other traditional de-noising methods, the proposed method in this paper has higher PSNR value, that is, the effect is better. And the image edge details of the algorithm is clear, and the subjective visual effect is better than others.

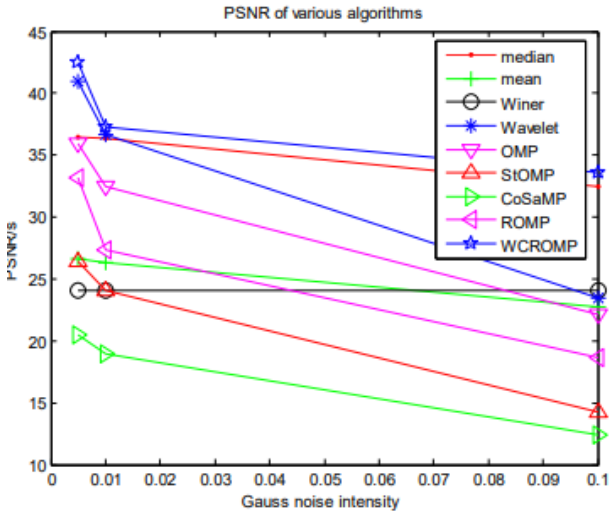

(A)

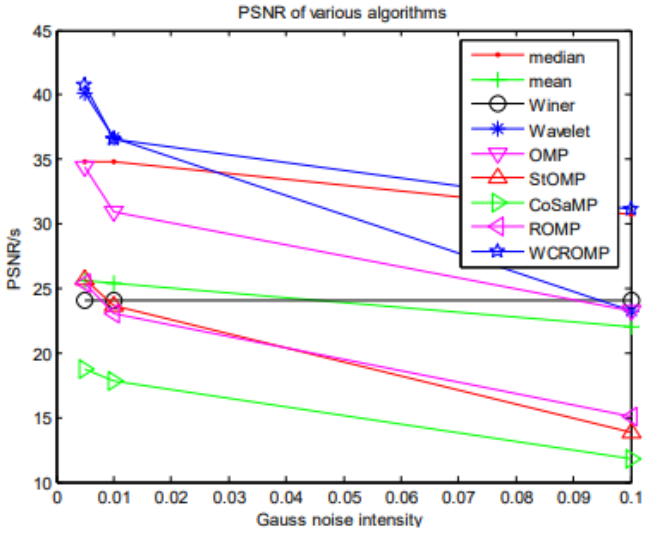

(B)

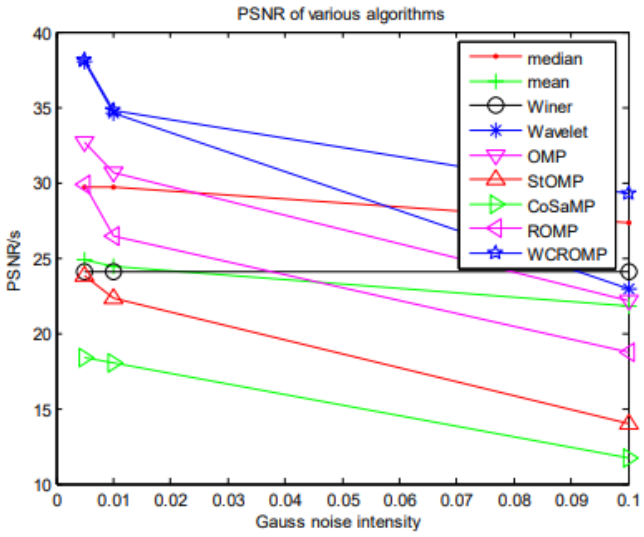

(C)

Fig. 8. The PSNR comparison curve obtained by using various de-noising algorithms(A)The PSNR curve of scratch image (B) The PSNR curve of scar image (C) The PSNR curve of surface upwarping image

5. Conclusion

For cold-rolling complex environment, and its images in the acquisition, acquisition, transfer process will be polluted by visible or invisible noise, we focus on de-noising method based on the improved compressive sensing algorithm. The conclusions are as follows:

(1) Various filtering algorithms have inhibitory effect on the strip surface defects of Gauss noise and salt & pepper noise;

(2) For the ROMP algorithm, the PSNR value and the running time of the image are affected by different sampling rate. Considering the two, the optimal sampling rate is 0.5.

(3) Compared with the traditional filtering methods, WCROMP algorithm has a better filtering effect in this paper, the PSNR value is higher, and the image edge information and details more clearly;

(4) Under the same noise intensity, the proposed algorithm has a little difference on the de-noising effect for different kinds of defects.

(5) Compared with the traditional compressive sensing algorithm such as OMP, StOMP , CoSaMP and ROMP , the proposed method has better de-noising effect.

The next step is focused on its universality and adaptability, and how to solve the problem of long time operation.

References

[1] Donoho D L. "De-noising by soft-thresholding", *IEEE Transaction on Information Theory* 41(3) (1995): 613-627.

[2] Portilla J., Strela V.,Wainwright M J.,Semoncelli EP. "Image de-noising using scale mixtures of Gaussians in the wavelet domain ", *IEEE Transactions on Image Processing*12(11)(2003): 1338-1351.

[3] Weiwei Liu, Yan Yun-hui, Sun Hong-wei Zhang Yao, Wu Yan-ping." Impulse noise reduction in surface defect of steel strip images based on neighborhood evaluation", *Chinese Journal of Science Instrument* 29(9) (2008): 1846-1850.

[4] Weiwei Liu, Yan Yun-hui, Li Zhan-yu, Li Jun. "An image filtering algorithm for online detection system of steel strip surface defects", *Journal of Northeastern University (Natural Science)* 30(3) (2009): 430-433.

[5] Bo Tang, Kong Jian-yi, Wang Xing-dong Jiang Guo-zhang, Xiong Hegen, Yang Jin-tang. "Wavelet threshold denoising for steel strip surface defect image", *Journal of Wuhan University of Science and Technology*, 33(1) (2010): 38-42.

[6] Yunhui Yan, Peng Yishu. "Removing impulse noise from surface defect images of steel strip based on threshold theory", *Journal of Northeastern University (Natural Science)* 31(5) (2010): 717-720.

[7] Hao Xu. "Image processing and identification of strip steel surface defects based on machine vision", *Thesis for master's degree of Wu Han University of science and technology* (2012).

[8] Amin Tavakoli, Ali Pourmohammad. "Image Denoising Based on Compressed Sensing", *International Journal of Computer Theory and Engineering* 4(2) (2012): 266-269.

[9] Zhang Shunli." Compressed Sensing Method Application in Image Denoising", *International Journal of Signal Processing, Image Processing and Pattern Recognition* 8(1) (2015): 203-212.

[10] M. T. Alonso, P. L. Dekker, J. J. Mallorqui. "A Novel Strategy for Radar Imaging Based on Compressive Sensing', *IEEE Transaction Geoscience and Remote Sensing* 48(12) (2010): 4285-4295.

[11] D Donoho. "Compressed sensing ", *IEEE Transaction on Information Theory* 52(4) (2006): 1289-1306.

[12] D Donoho, Y Tsaig. "Extensions of compressed sensing ", Signal *Processing* 86(3) (2006): 533-548.

[13] Michael Elad. "Sparse and Redundant Representations". London*; Springer Science* (2010).

[14] J Tropp A Gibert. "Signal recovery from random measurements via orthogonal matching pursuit", *IEEE Transaction on Information Theory* 53(12) (2008): 4655-4666.

[15] E. Candes, J. Romberg. "Sparsity and incoherence in compressive sampling ", *Inverse Problems*, 23(3) (2007): 969-985.

[16] E. Candes, J. Romberg, T. Tao. "Robust uncertainty principles: Exact signal reconstruction from highly incomplete frequency information ", *IEEE Transaction on Information Theory* 52(2) (2006): 489-509.

[17] E. Candes, J. Romberg, T. Tao. "Stable signal recovery from incomplete and inaccurate measurements", *Communications on Pure Applied Mathematics* 59(8) (2005): 1207-1223.

[18] Figueiredo M A T, Nowak R D, Wright S J. "Gradient projection for sparse reconstruction: Application to compressed sensing and other inverse problems", *Journal of Selected Topics in Signal Processing: Special Issue on Convex Optimization Methods for Signal Processing* (194) (2007): 586-598.

[19] Needell D，VershyninR. "Uniform uncertainty principle and signal recovery via regularized orthogonal matching pursuit", *Foundations of Computational Mathematics* 9(3) (2009): 317-334.

[20] Needell D，Vershynin R． "Signal recovery from incomplete and inaccurate measurements via regularized orthogonal matching pursuit", *IEEE Journal on Selected Topics in Signal Processing* 4(2) (2010): 310-316.

[21] Zhen-zhen Yang, Yang Zhen, Sun Lin-hui. "A Survey on Orthogonal Matching Pursuit Type Algorithms for Signal Compression and Reconstruction", *Journal of Signal Processing* 29(4) (2013): 486-496.